Integrin-dependence of extramedullary erythropoiesis in the spleen of *Jak2-V617F* positive myeloproliferative neoplasm in mice

Conny K. Baldauf[a,b,*], Linda Poschmann[b,c,*], Bärbel Edelmann-Stephan[c,1], Frank Angenstein[d], Tobias R. Haage[c], Vikas Bhuria[c], Lars Philipsen[a], Hannes Berlin[a], Daniela C. Dieterich[e], Martin Böttcher[b,c], Dimitrios Mougiakakos[b,c,f], Burkhart Schraven[a,b,f], and Thomas Fischer[b,c,f#]

[a]*Institute for Molecular and Clinical Immunology, Otto-von-Guericke University, Medical Faculty, Magdeburg, Germany;* [b]*Healthcampus Immunology, Inflammation and Infectiology (GC-I[3]);* [c]*Department of Hematology, Oncology and Cell Therapy, Otto-von-Guericke University, Medical Faculty, Magdeburg, Germany;* [d]*German Center for Neurodegenerative Diseases (DZNE), Otto-von-Guericke University, Magdeburg, Germany;* [e]*Institute for Pharmacology and Toxicology, Otto-von-Guericke University, Medical Faculty, Magdeburg, Germany;* [f]*Center for Health and Medical Prevention – CHaMP, Otto-von-Guericke University Magdeburg, Germany*

The molecular mechanisms driving splenomegaly in myeloproliferative neoplasms (MPNs) remain poorly understood. Utilizing the *Jak2-V617F* knock-in mouse model, we investigated the role of β1- and β2-integrins in regulating spleen volume and spleen weight. The response to neutralizing antibodies against VLA-4 and the β2-integrin chain, as well as to isotype controls, was evaluated by serial intraindividual magnetic resonance imaging, by assessment of spleen weight and by analysis of the cellular composition of spleens. Short-term anti-VLA-4/β2-integrin treatment (applied on day 1 and evaluated at day 8) significantly reduced the spleen volume by 30% compared with the immunoglobulin G (IgG) control. At the cellular level, anti-integrin treatment led to a substantial 30% decrease in erythroblast counts and a 23% reduction in basophilic erythroblasts within the spleen, as compared with the isotype control. Furthermore, immunohistochemistry analysis of spleen sections revealed that CD71 (= Transferrin receptor protein 1) expression in spleen remained largely unchanged, whereas there was a clear reduction in Ter119 expression upon anti-integrin treatment. These data suggest that the substantial decrease in erythroblasts following anti-integrin treatment is a primary factor contributing to the overall reduction in spleen size. To study the spleen architecture, multiepitope ligand cartography (MELC) analysis of spleen sections was applied. This demonstrated that the spatial distribution of the marginal zone, red pulp, and white pulp remained unaltered upon anti-integrin treatment in JAK2-V617F knock-in mice. In summary, the present study identified a previously unrecognized role of the β1-integrin VLA-4 and of β2-integrin chains in extramedullary erythropoiesis of the spleen in JAK2-V617F-induced disease. © 2025 The Authors. Published by Elsevier Inc. on behalf of International Society for Experimental Hematology. This is an open access article under the CC BY license (http://creativecommons.org/licenses/by/4.0/)

HIGHLIGHTS

- Blockage of VLA4/β2-integrins in *Jak2*$^{+/V617F}$ mice reduced spleen volume and weight
- Spleen erythroid hyperplasia was also reduced by anti-integrin treatment
- Multiepitope ligand cartography (MELC) analysis revealed that the spleen architecture was unchanged

Polycythemia vera (PV) is one of the classic Philadelphia chromosome–negative myeloproliferative neoplasms (MPNs) characterized by a somatic *JAK2-V617F* mutation [1–3]. The approval of JAK inhibitors improved the morbidity of patients with MPN, primarily by reducing inflammatory constitutional symptoms and splenomegaly [4–6]. Splenomegaly observed in patients with PV and in *Jak2-V617F* knock-in mice is characterized by marked erythroid hyperplasia [7,8]. There is complete effacement of the white pulp (WP) and abnormal accumulation of CD71$^+$ Ter119$^+$ erythroblasts [8]. Although the cel-

*CKB and LP contributed equally to this study and share the first authorship.
[1]Present address: DLR-Projektträger, Heinrich-Konen-Straße 1, Bonn, Germany
Address correspondence to Thomas Fischer, MD, Department of Hematology, Oncology and Cell Therapy, Medical Center, Otto-von-Guericke University, Leipziger Strasse. 44, 39120 Magdeburg, Germany; E-mail: thomas.fischer@med.ovgu.de

0301-472X/© 2025 The Authors. Published by Elsevier Inc. on behalf of International Society for Experimental Hematology. This is an open access article under the CC BY license (http://creativecommons.org/licenses/by/4.0/)

https://doi.org/10.1016/j.exphem.2025.105340

lular changes associated with *Jak2-V617F*-induced splenomegaly are well described, there are almost no data on the molecular mechanisms regulating this pathophysiologic process. Interestingly, in healthy wild-type mice, it has been reported that the β1- and β2-integrins VLA-4 and LFA-1 play an essential role in lymphocyte migration into the splenic WP [9]. Integrins are transmembrane heterodimers, each consisting of one α-subunit and one β-subunit. The major β1 integrin VLA-4 (=$\alpha_4\beta_1$) binds to the adhesion molecule VCAM-1 and is expressed on a wide spectrum of hematopoietic cells, including stem cells, erythroblasts, and leukocytes [10,11]. Integrin β2 (=CD18) is the β-chain of 4 integrin heterodimers: $\alpha_L\beta_2$ (LFA-1), $\alpha_M\beta_2$ (Mac-1), $\alpha_X\beta_2$, and $\alpha_D\beta_2$. [12]. The β2-integrins are primarily expressed on leukocytes, however, $\alpha_L\beta_2$ (LFA-1), $\alpha_M\beta_2$ (Mac-1) are also expressed on erythroblasts [13]. Integrins play a pivotal role in communication and adhesion of hematopoietic cells and in inflammatory conditions [14].

Previously, we and others demonstrated that JAK2-V617F leads to aberrant activation of β1 and β2-integrins on human and mouse hematopoietic cells, resulting in enhanced adhesion and decreased motility. [15–18]. For β1 integrins, as VLA-4, this is achieved by a JAK2-V617F-induced structural change from the bent low-affinity to the open high-affinity conformation. [17]. Translocation of the small GTPase Rap1 from the cytosol to the inner leaflet of the plasma membrane is involved [17]. Here, we investigated whether JAK2-V617F-induced dysregulation of β1- and β2-integrins contributes to formation of splenomegaly in *Jak2-V617F* knock-in mice. Blockade of VLA-4 and β2-integrins by anti-integrin antibody treatment was employed. Splenomegaly in *Jak2-V617F* knock-in mice was monitored using serial magnetic resonance imaging (MRI) of spleen volumes. In addition, the changes in spleen weight and in the splenic composition of erythroblasts, granulocytes, and hematopoietic progenitors were characterized.

METHODS

Mouse Model and Antibody Injections

The Vav1-Cre *Jak2-V617F* mouse, a conditional hematopoiesis-specific *Jak2-V617F* knock-in model, has been described previously. [8,15,17]. Nine-week-old Vav1-Cre $Jak2^{VF/+}$ mice ($Jak2^{VF/+}$) were injected intraperitoneally with 200 μg each of anti-VLA-4 and anti-β2-integrin antibodies (dissolved in a total of 200 μL phosphate-buffered saline [PBS]) or the corresponding immunoglobulin G (IgG) isotype control antibodies (200 μg of each isotype control; dissolved in a total of 200 μL PBS) on day 1 and day 8. The antibody clones used, the route of administration, and the dose of anti-integrin antibodies have been described previously [17,19]. Specifics of antibodies are listed in Supplementary Table E1A. Mice were sacrificed on day 8 (single injection) or day 15 (double injection). Spleens, bone marrow, and peripheral blood were analyzed. In addition, a second set of experiments was performed where $Jak2^{+/+}$ and $Jak2^{VF/+}$ mice were injected with PBS (control), anti-VLA-4/β2-integrin antibodies, and isotype IgG, respectively, only once on day 1. Animal studies were approved by the government authority of Saxony-Anhalt, Germany, under registration number 42502-2-1496.

Small Animal MRI

A 4.7 T small animal MRI scanner (Bruker Biopec 47/20, Bruker BioSpin GmbH) and ParaVision 4.0 were used for MRI imaging to analyze spleen volume during antibody treatments. T2-weighted images were acquired on days 1, 8, and 15 using the rapid acquisition relaxation-enhanced (RARE) sequence. The following parameters were used: TR 3500 msec, TE 12 msec, layer thickness 2 mm, image size 30 × 30 mm, matrix 128 × 128, RARE-factor 8, averaging 8, total measuring time 5 min, 36 sec. Raw data were analyzed using ImageJ.

Spleen Weight Assessment

Mice were euthanized by cervical dislocation. Spleens were carefully excised from each animal and immediately assessed. The wet weight of each spleen was determined using a precision analytical balance (Kern EMB, Kern, & Sohn GmbH) and recorded in milligrams (mg).

Flow Cytometry Analysis

Immunophenotyping by flow cytometry was performed using a FACSCanto II (BD Biosciences). Antibodies used are listed in Supplementary Table E1B. Samples were stained for 15 minutes at room temperature and washed with 1 mL PBS +1% fetal calf serum.

Multiepitope Ligand Cartography

Multiepitope ligand cartography (MELC) was performed according to Edelman et al. [17] on isolated spleen sections of anti-VLA-4/β2-integrin antibody, IgG isotype control, or PBS-treated mice. Analyses were performed in a blinded manner with artificial intelligence (AI) assistance. Antibodies used are indicated in Supplementary Table E1B.

Statistics

Statistical analysis was carried out using GraphPad Prism (version 9). Data are shown as mean ± SEM. The particular test used is indicated in the respective figure legend.

RESULTS AND DISCUSSION

To investigate the role of integrins in in vivo formation of JAK2-V617F-induced splenomegaly, young 9-week-old mice were treated with anti-VLA-4/β2-integrin antibodies and isotype IgG control antibodies, respectively, on day 1 and day 8 (Figure 1A). In young mice of this age, splenomegaly is still developing and has not reached its final size. Small animal MRI was used to intraindividually assess spleen volumes on days 1, 8, and 15 during treatment with anti-VLA4-/β2-integrin or IgG isotype control (Figure 1A). Anti-VLA-4/β2-integrin treatment significantly reduced the spleen volume by a mean of 30.3% and 30.8% on days 8 and 15, respectively, as compared with the IgG control (Figure 1A). Representative images of one frontal plane of $Jak2^{VF/+}$ mice treated with anti-VLA-4/β2-integrin antibodies or IgG isotype controls are shown in Figure 1B. In a second set of experiments, $Jak2^{+/+}$ and $Jak2^{VF/+}$ mice were treated with anti-integrin antibodies, with PBS vehicle and with isotype IgG once on day 1 and spleen weight was measured on day 8 (Figure 1C). Notably, in $Jak2^{+/+}$ control mice no effect of anti-VLA-4/β2-integrin treatment was observed (Figure 1C). In $Jak2^{VF/+}$ mice there was a statistically significant decrease in spleen weight upon anti-VLA-4/β2-integrin treatment in comparison to vehicle control, whereas the comparison of anti-integrin treatment versus isotype IgG did not reach

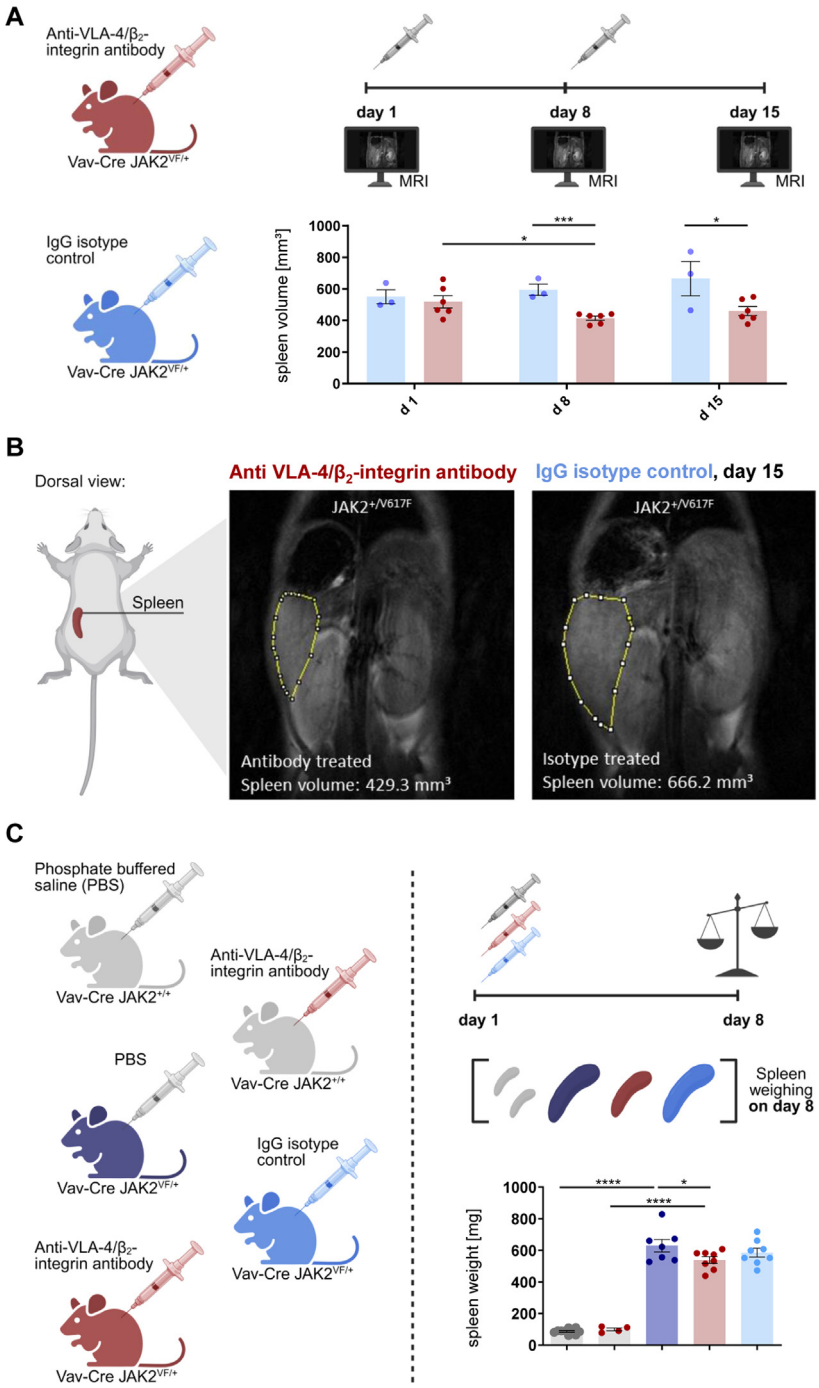

Figure 1 Spleen volume and spleen weight of *Jak2*$^{VF/+}$ knock-in mice are significantly decreased upon treatment with anti-VLA-4/β2-integrin antibodies. **(A)** Spleen volume was determined by serial small animal MRI on days 1, 8, and 15. Anti-VLA-4/β2-integrin antibodies (each 200 μg; n = 6) or IgG isotype controls (each 200 μg; n = 3) were injected intraperitoneally on days 1 and 8. The spleen volume was analyzed by frontal and horizontal plane measurements using ImageJ. At the start of the experiment, mean spleen volumes were similar in the cohorts of isotype treated *Jak2*$^{VF/+}$ mice (indicated in light blue) and anti-VLA-4/β2-integrin antibody treated mice (indicated in red): 550 $\pm$ 44 mm^3 and 518 $\pm$ 39 mm^3 (mean $\pm$ standard error of mean [SEM]), respectively. On day 8 a significant reduction in spleen volume from 595 $\pm$ 36 mm^3 in the isotype control group to 414 $\pm$ 13 mm^3 in the anti-VLA-4/β2-integrin antibody group (***p = 0.0006; unpaired t test) was observed. On day 15 of treatment, the decrease in spleen volume was from 665 $\pm$ 108 mm^3 to 460 $\pm$ 28 mm^3 (*p = 0.0410; unpaired t test). In the anti-VLA-4/β2-integrin antibody treated group, the decrease in mean spleen volume from baseline to day 8 was from 518 $\pm$ 39 mm^3 (mean $\pm$ SEM) to 414 $\pm$ 13 mm^3 (*p = 0.0302; unpaired t test) and to 460 $\pm$ 28 mm^3 on day 15. Cartoon created with Biorender.com (https://biorender.com/k22j077). **(B)** Representative images of one

statistical significance. Nevertheless, a trend toward a decrease of spleen weight in the latter analysis was observable. The slightly different outcome in comparison with the MRI study is likely attributable to differences in the method of recording spleen parameters: volume versus weight, intravital analysis versus postmortem analysis, and intraindividual MRI analysis versus analysis of weight in different cohorts of mice. In addition, the smaller effect may be due not only to the different measurement method, but also because the mice in this experiment were treated only once on day 1. In Figure 1A, the greatest effect is seen after 2 treatments (day 1 and day 8) on day 15.

Recently, Austin et al. [20] reported that treatment with peg-IFN-α weekly for 4 weeks has demonstrated a 30% reduction in the mean spleen weight of JAK2-V617F knock-in mice. However, 4 weeks of ruxolitinib treatment using WT/*Jak2*$^{VF/+}$ chimeric mice resulted in a strong decrease in spleen weight from a mean of approximately 300 mg to 100 mg in vehicle-treated mice [20]. Interestingly, in the pivotal COMFORT-I trial in myelofibrosis, Verstovsek et al. [4] reported reduction in spleen volume of 35% or more at 24 weeks, assessed by MRI, in 41.9% of patients in the ruxolitinib group as compared with 0.7% in the placebo group. In a recent review, similar response rates for splenomegaly in myelofibrosis were reported for other JAK inhibitors [21]. In JAK2-V617F knock-in mice used in this study, reticulin fibrosis is absent in both *Jak2*$^{VF/+}$ bone marrow and spleen, even in mice that are 6 months old [8]. Therefore, to study the effects of anti-integrin treatment in myelofibrosis, further research in MPN mouse models developing fibrosis is warranted.

Next, we aimed to determine the role of VLA-4 and of the β2-integrins in the cellular composition of splenomegaly. Because the MRI study has shown the most significant change in spleen size at day 8 (Figure 1A), a single injection of anti-integrin antibodies was used on day 1 and mice were sacrificed on day 8. PBS- and IgG-treated *Jak2*$^{VF/+}$ mice were included as controls. The rationale for employing PBS treatment as an additional control was based on the concern that high-dose IgG (as utilized for the isotype control) may modulate the inflammatory splenic microenvironment of *Jak2*$^{VF/+}$ mice, thereby introducing an experimental bias. Indeed, the immunomodulatory activity of high-dose IgG has been described, including the suppression of IL-1- and TNFα-mediated mechanisms [22,23].

First, eythroblasts were analyzed using Ter119 as an erythroid lineage marker. Erythropoietic cells display VLA-4, LFA-1, and Mac-1, which are regulated differentially depending on the stage of maturation [24]. As reported by Mullally et al. [8] previously, the spleen of *Jak2*$^{VF/+}$ knock-in mice showed strongly increased erythroblast counts as compared with *Jak2*$^{+/+}$ mice (Figure 2C, left panel). Remarkably, although anti-integrin treatment did not change the erythroblast composition in bone marrow (Figure 2B), strong reduction in spleen erythroblasts was noted upon anti-integrin antibody treatment (Figure 2C, left panel). This was observable both in comparison with the PBS-treated control and the isotype control and reached a significant 30% reduction of spleen erythroblast counts when compared with the isotype control cohort (Figure 2C, left panel). We then investigated the involvement of integrins in dysregulated erythroid differentiation. Upon anti-integrin treatment, a significant reduction of basophilic erythroblasts (RII) [25] in the spleen was observed when compared both with the PBS control and the isotype control (23% reduction) (Figure 2C, right panel). RI and RIII erythroblasts did not show significant changes (data not shown). To control for erythroblast abundance in situ, we used immunohistochemistry on spleen sections (Figure 2D). This showed that CD71 (= transferrin receptor protein 1) expression remained largely unchanged, whereas there was a clear reduction in Ter119 expression following anti-integrin treatment compared with IgG control (Figure 2D), consistent with a reduction in basophilic erythroblasts. This is in line with the results obtained by FACS analysis depicted in Figure 2C.

Mechanistically, the changes in erythroblast composition observed in spleen of anti-VLA-4/β2-integrin antibody–treated *Jak2*$^{VF/+}$ mice are consistent with strong VLA-4 and β2-integrin expression on erythroblasts [10]. Interestingly, the high VLA-4 expression on erythroblasts decreases during differentiation, whereas expression of the β2-integrins LFA-1 and Mac-1 increases [10,11]. This underlines the usefulness of the here applied combination of anti-VLA-4 and anti-β2-chain antibody treatment. VLA-4 mediates the adhesion of erythroblasts to fibronectin, thereby promoting erythroblast expansion [11]. Incubation of CD71$^+$ or Ter119$^+$ wild-type cells with neutralizing anti-VLA-4 antibody was reported to strongly inhibit their homing to hematopoietic tissues compared with the IgG control [10]. Furthermore, it is conceivably that increased adhesion induced by the *Jak2-V617F*-activated VLA-4 and β2-integrins [15–17] translates in increased homing, thereby promoting extramedullary erythropoiesis in spleen.

Next, we analyzed the cellular composition in granulocytes and in hematopoietic stem and progenitor cell (HSPC) populations in the spleen upon anti-VLA-4/β2-integrin antibody treatment. Again, a single injection of anti-integrin antibodies was employed on day 1 and mice were sacrificed on day 8. As compared with IgG control, this analysis revealed no significant changes in HSPC populations whereas spleen granulocytes showed a decrease in comparison with the PBS control (Figure 3B, C). Hematocrit, red blood cell (RBC), white blood cell (WBC), and platelet (PLT) counts in peripheral blood were not downregulated upon short-term anti-integrin treatment (Figure 3D–G). The absence of a decrease in RBC and hematocrit

frontal plane of *Jak2*$^{VF/+}$ mice treated with anti-VLA-4/β2-integrin antibodies or IgG isotype controls are shown. The spleen circumference is highlighted in yellow. Cartoon created with Biorender.com (https://biorender.com/f07s746). **(C)** In a second set of experiments, mice were treated on day 1 with PBS (control), anti-VLA-4/β2-integrin antibodies and IgG isotype, respectively. On day 8, mice were sacrificed and the spleen weight was measured. There was no apparent change in spleen weight of anti-VLA-4/β2-integrin antibody–treated WT *Jak2*$^{+/+}$ mice (n = 4) when compared with PBS-treated WT *Jak2*$^{+/+}$ mice (n = 10). Compared with the *Jak2*$^{+/+}$ mice (n = 10; mean spleen weight: 87.3 ± 5 mg), Vav1-Cre *Jak2*$^{VF/+}$ mice (n = 7) exhibited a significantly higher spleen weight (629.3 ± 39 mg; ****$p < 0.0001$). This was significantly reduced by the anti-VLA-4/β2-integrin antibody treatment (n = 8; 538.8 ± 20 mg; *$p = 0.0163$). Mean spleen weight of IgG isotype–treated Vav1-Cre *Jak2*$^{VF/+}$ mice (n = 8) was 585.8 ± 27 mg. The comparison anti-integrin treatment versus isotype IgG did not reach a statistically significant difference. However, there was a trend ($p = 0.16$) toward a decrease of spleen weight in the anti-integrin–treated Vav1-Cre *Jak2*$^{VF/+}$ mice. Data are shown as mean ± SEM. Ordinary one-way analysis of variance was used. Cartoon created with Biorender.com (https://BioRender.com/tnmjiva). *WT* = wild-type.

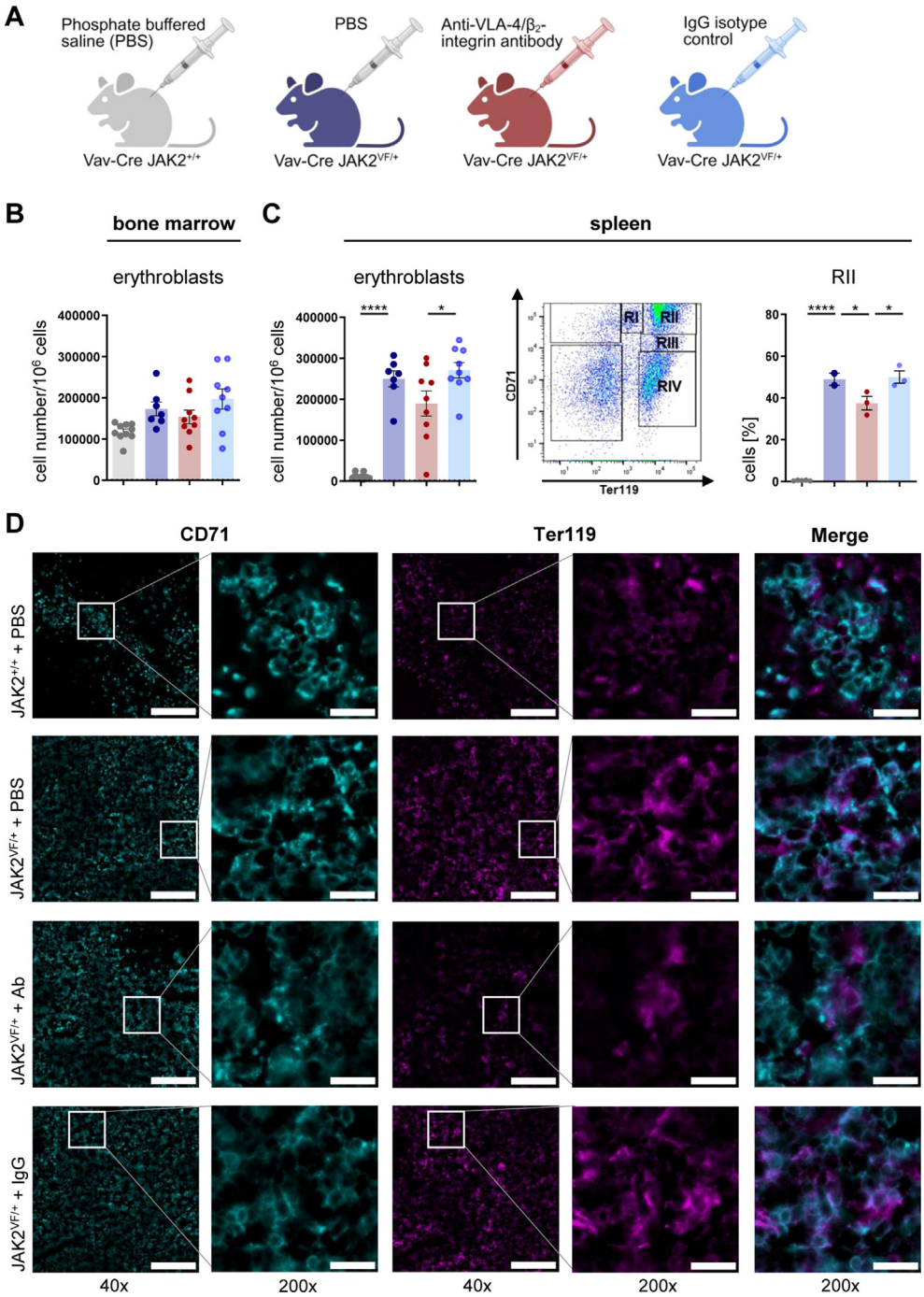

Figure 2 Cell composition in erythroblasts of the spleen in *Jak2*$^{+/+}$ and *Jak2*$^{VF/+}$ knock-in mice. The experimental design is shown in **(A)** (Created with Biorender.com, https://biorender.com/f0h8rw1). *Jak2*$^{+/+}$ (gray) and *Jak2*$^{VF/+}$ (dark blue) mice were injected intraperitoneally on day 1 with 200 μL PBS (controls). Additional cohorts of *Jak2*$^{VF/+}$ mice were injected on day 1 with anti-VLA-4/β2-integrin antibody (red) and IgG isotype control (light blue) (each 200 μg in a total volume of 200 μL) (n = 7–10). On day 8, mice were sacrificed and erythroblasts in bone marrow and spleen were measured. Erythroblasts shown as mean ± standard error of mean (SEM) were measured by FACS and normalized to 1 × 10^6 **(B)** bone marrow cells and **(C**, left panel**)** spleen cells. (**C**, middle panel) Erythrocyte differentiation was analyzed by FACS according to the CD71-Ter119 classification of Socolovsky et al. [25]. The percentages of pro-erythroblasts (RI), basophilic erythroblasts (RII), and polychromatic erythroblasts (RIII) were measured as % of total spleen cells. **(C**, right panel and data not shown**).** Composition in basophilic erythroblasts (RII) is shown as mean ± SEM. For **(B)** and **(C)** ordinary one-way analysis of variance was used); *$p < 0.05$, ****$p < 0.001$. **(D)** Immunohistochemistry obtained by MELC analysis on spleen sections of *Jak2*$^{+/+}$ and *Jak2*$^{VF/+}$ mice injected intraperitoneally with 200 μL PBS (controls) and of *Jak2*$^{VF/+}$ mice upon treatment with

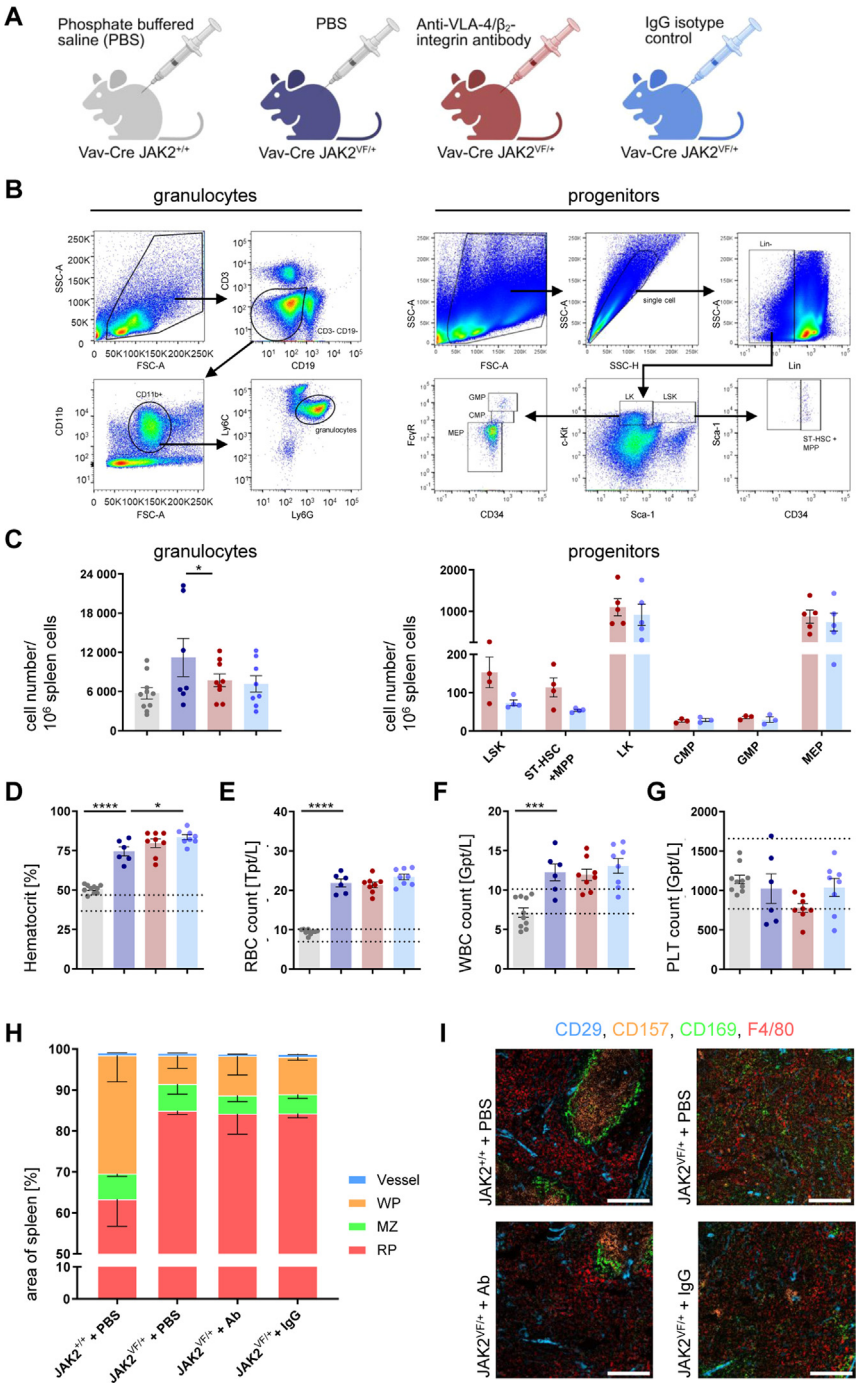

Figure 3 Cell composition in granulocytes and in HSPC of the spleen and spleen architecture of *Jak2*$^{+/+}$ and *Jak2*$^{VF/+}$ knock-in mice. The experimental design is shown in **(A)** (Created with Biorender.com, https://biorender.com/f0h8rw1). *Jak2*$^{+/+}$ (grey) and *Jak2*$^{VF/+}$ (dark blue) mice were injected intraperitoneally on day 1 with 200 μl PBS (controls) (n = 6–10). Additional cohorts of *Jak2*$^{VF/+}$ mice were injected on day 1 with anti-VLA-4/β2-integrin antibody (red) and IgG isotype control (light blue) (each 200 μg in a total volume of 200 μL) (n = 8). On day 8, mice were sacrificed and analyzed **(C–I). (B)** Gating scheme of flow cytometric data for the analysis of

anti-VLA-4/β2-integrin antibodies (Ab) and isotype IgG control, respectively. Representative images of CD71 (turquoise) and Ter119 (pink) expression in spleen sections are shown at $\times$40 and $\times$200 magnification with a scale bar of 100 and 20 μm, respectively. The merged image shows CD71 (turquoise) and Ter119 (pink) to indicate the localization of expression.

upon anti-integrin treatment is in line with results by the Papayannopoulou laboratory demonstrating that mice lacking the β1-integrin have normal hematocrit under steady state conditions but are unable to respond to erythroid stress [26].

The normal splenic structure is divided into three distinct zones: the white pulp (WP), red pulp (RP), and marginal zone (MZ). To study the spleen architecture in sections from both anti-integrin antibody–treated and isotype control mice, MELC analysis was applied. Different zones are characterized by different cell populations and their expression markers. Using an AI-assisted algorithm based on the spatial distribution of CD157 (WP marker [27]), CD169 (splenic MZ macrophages [28]), F4/80 (marker for macrophages within the RP [29]), CD29 (integrin β1, used as endothelial marker [30]), and propidium iodide, we monitored the distribution of MZ, WP, RP, and vessels in a semiquantitative way (Figure 3H). This analysis revealed that the strong increase in the RP area was basically unchanged upon anti-integrin or isotype IgG treatment in *Jak2*$^{VF/+}$ mice (Figure 3H, I). In summary, the reduction in spleen volume was in line with the reduction in the erythroblast content in spleen after anti-integrin treatment (Figure 2C). Thus, the significant reduction in erythroblasts appears as a main contributor for the overall reduction in spleen size. In conclusion, our study identifies a previously unrecognized role of the β1-integrin VLA-4 and of β2-integrin chains in extramedullary erythropoiesis in the spleen of JAK2-V617F-induced disease. In addition, our results offer exploration of novel therapeutic targets in MPN. However, the most efficient schedule in terms of antibody dosing, duration of treatment, and a potential combination with JAK inhibitors need to be investigated in future studies and was beyond the scope of this explorative investigation.

Declaration of competing interest

LP is a Dr. med. candidate at the Otto-von-Guericke University Magdeburg. The authors do not have any conflicts of interest to declare in relation to this work.

Acknowledgments

Partly presented in abstract form at the 60th annual meeting of the American Society of Hematology, December 2018.

Author Contributions

T.F., Linda P., C.K.B., and B.E.S. designed the project; C.K.B. and T. F. wrote the manuscript with support of all authors; Linda P., C.K.B., F.A., T.R.H., V.B., Lars P., and H.B. performed experiments; T.R.H. contributed through generation of figures; D.C.D., M.B., D.M., and B. S. analyzed data and discussed and interpreted results.

Data Availability

Original data and protocols are obtainable from the corresponding author upon a reasonable request.

Funding

The project was supported by research funding from German Research Council (Deutsche Forschungsgemeinschaft [DFG]), 97850925/SFB854/A20 to T.F. and B19 to B.S.. L. Poschmann was funded by an MD fellowship from the German Research Foundation (DFG), 97850925/SFB854. B.S. was funded by grants of the state of Saxony-Anhalt (projects SI 2 and SI 3, respectively). T.R.H. was funded by grant 361210922/RTG 2408 of the German Research Foundation (Deutsche Forschungsgemeinschaft, DFG). T.F. is funded by a donation from the Wellhoeferstiftung, Germany.

SUPPLEMENTARY MATERIALS

Supplementary material associated with this article can be found online at https://doi.org/10.1016/j.exphem.2025.105340

HSPC. **(C**, left panel**)** Spleen granulocytes and **(C**, right panel**)** HSPC composition in the spleen were measured by FACS and normalized to 1 $\times$ 10^6 spleen cells. LSK cells, short-term hematopoietic stem cells (ST-HSCs), multipotent progenitor cells (MPPs), LK cells, common myeloid progenitor cells (CMPs), granulocyte/monocyte progenitor cells (GMPs), and megakaryocyte/erythroid progenitor cells (MEPs) were examined. Regardless of the statistical analysis employed (Mann–Whitney *U* test, two-way analysis of variance (ANOVA) Sidak's multiple comparison test), no statistically significant findings were identified in the HSPC analysis. Some of the mice were not used for analysis because the selected cutoff of 100 cells per gate was not met for some cell populations. **(D–G)** Peripheral blood cell counts from PBS-injected *Jak2*$^{+/+}$ (gray) and *Jak2*$^{VF/+}$ mice (dark blue) (controls) and anti-VLA-4/β2-integrin antibodies (red) or IgG isotype control (light blue)-treated *Jak2*$^{VF/+}$ mice. **(D)** hematocrit, **(E)** RBC count, **(F)** WBC count, and **(G)** PLT count. Data are shown as mean $\pm$ SEM. For **(C**, left panel**)** and **(D–G)** one-way ANOVA with Tukey's multiple comparisons test was used. For **(C**, right panel**)** Mann–Whitney *U* test was performed. *$p < 0.05$, ***$p < 0.001$, ****$p < 0.0001$. **(H)** Spleen structure was analyzed using MELC analysis and an AI-based algorithm (based on different fluorescent markers) of *Jak2*$^{+/+}$ + PBS (n = 5), *Jak2*$^{VF/+}$ + PBS (n = 3), *Jak2*$^{VF/+}$ + anti-VLA-4/β2-integrin antibody treatment (Ab; n = 3) and *Jak2*$^{VF/+}$ + IgG isotype control (IgG; n = 3) treated mice was applied. A single injection of anti-integrin antibodies/isotype IgG/PBS vehicle was employed on day 1 and mice were sacrificed on day 8. We used the pixel classification workflow of Ilastic toolbox [https://pubmed.ncbi.nlm.nih.gov/31570887/] for the automated segmentation of measured field of view into region of interest (ROI) of white and RP, MZ and vessel structures. Therefore, we selected the images of the marker CD29 (vessels), F4/80 (RP), CD157 (WP), CD169 (MZ), and propidium iodide (nuclei) of a wild-type spleen section to train the random forest network. The recall of this classifier network results in the four ROIs (RP and WP, MZ, vessels) for each field of view. Please refer to Supplementary Table E1B for a list of the antibodies used. **(I)** Immune histology of representative spleen sections obtained from mice treated as indicated. The expression of CD29, CD157, CD169, and F4/80 was used to mark the vessels (blue), the WP (orange), the MZ (green), and the RP (red), respectively. The colors represent the corresponding markers in the representative merged images shown in **(I)**. The scale bar represents 200 μm.

REFERENCES

1. James C, Ugo V, Le Couédic JP, et al. A unique clonal JAK2 mutation leading to constitutive signalling causes polycythaemia vera. Nature 2005;434:1144–8. https://doi.org/10.1038/nature03546.
2. Kralovics R, Passamonti F, Buser AS, et al. A gain-of-function mutation of JAK2 in myeloproliferative disorders. N Engl J Med 2005;352:1779–90. https://doi.org/10.1056/NEJMoa051113.
3. Levine RL, Wadleigh M, Cools J, et al. Activating mutation in the tyrosine kinase JAK2 in polycythemia vera, essential thrombocythemia, and myeloid metaplasia with myelofibrosis. Cancer Cell 2005;7:387–97. https://doi.org/10.1016/j.ccr.2005.03.023.
4. Verstovsek S, Kantarjian H, Mesa RA, et al. Safety and efficacy of INCB018424, a JAK1 and JAK2 inhibitor, in myelofibrosis. N Engl J Med 2010;363:1117–27. https://doi.org/10.1056/NEJMoa1002028.
5. Harrison C, Kiladjian JJ, Al-Ali HK, et al. JAK inhibition with ruxolitinib versus best available therapy for myelofibrosis. N Engl J Med 2012;366:787–98. https://doi.org/10.1056/NEJMoa1110556.
6. Duminuco A, Torre E, Palumbo GA, Harrison C. A journey through JAK inhibitors for the treatment of myeloproliferative diseases. Curr Hematol Malig Rep 2023;18:176–89. https://doi.org/10.1007/s11899-023-00702-x.
7. Prakash S, Hoffman R, Barouk S, et al. Splenic extramedullary hematopoietic proliferation in Philadelphia chromosome-negative myeloproliferative neoplasms: heterogeneous morphology and cytological composition. Mod Pathol 2012;25:815–27. https://doi.org/10.1038/modpathol.2012.33.
8. Mullally A, Lane SW, Ball B, et al. Physiological Jak2V617F expression causes a lethal myeloproliferative neoplasm with differential effects on hematopoietic stem and progenitor cells. Cancer Cell 2010;17:584–96. https://doi.org/10.1016/j.ccr.2010.05.015.
9. Lo CG, Lu TT, Cyster JG. Integrin-dependence of lymphocyte entry into the splenic white pulp. J Exp Med 2003;197:353–61. https://doi.org/10.1084/jem.20021569.
10. Hintze C, Ströbele C, Rüster B, et al. Erythrocytic precursor cells show potent shear stress resistant adhesion and home to hematopoietic tissue in vivo. Transfusion 2009;49:2122–30. https://doi.org/10.1111/j.1537-2995.2009.02241.x.
11. Eshghi S, Vogelezang MG, Hynes RO, Griffith LG, Lodish HF. $\alpha4\beta1$ Integrin and erythropoietin mediate temporally distinct steps in erythropoiesis: integrins in red cell development. J Cell Biol 2007;177:871–80. https://doi.org/10.1083/jcb.200702080.
12. Bouti P, Webbers SDS, Fagerholm SC, et al. $\beta2$ Integrin signaling cascade in neutrophils: more than a single function. Front Immunol 2021;11:619925. https://doi.org/10.3389/fimmu.2020.61992.
13. Miller BA, Antognetti G, Springer TA. Identification of cell surface antigens present on murine hematopoietic stem cells. J Immunol 1985;134:3286–90.
14. Hogg N, Patzak I, Willenbrock F. The insider's guide to leukocyte integrin signalling and function. Nat Rev Immunol 2011;11:416–26. https://doi.org/10.1038/nri2986.
15. Haage TR, Charakopoulos E, Bhuria V, et al. Neutrophil-specific expression of JAK2-V617F or CALRmut induces distinct inflammatory profiles in myeloproliferative neoplasia. J Hematol Oncol 2024;17:43. https://doi.org/10.1186/s13045-024-01562-5.
16. Gupta N, Edelmann B, Schnoeder TM, et al. JAK2-V617F activates $\beta1$-integrin-mediated adhesion of granulocytes to vascular cell adhesion molecule 1. Leukemia 2017;31:1223–6. https://doi.org/10.1038/leu.2017.26.
17. Edelmann B, Gupta N, Schnoeder TM, et al. JAK2-V617F promotes venous thrombosis through $\beta1/\beta2$ integrin activation. J Clin Invest 2018;128:4359–71. https://doi.org/10.1172/JCI90312.
18. Matsuura S, Thompson CR, Ng SK, et al. Adhesion to fibronectin via $\alpha5\beta1$ integrin supports expansion of the megakaryocyte lineage in primary myelofibrosis. Blood 2020;135:2286–91. https://doi.org/10.1182/blood.2019004230.
19. Vermeulen M, Le Pesteur F, Gagnerault MC, Mary JY, Sainteny F, Lepault F. Role of adhesion molecules in the homing and mobilization of murine hematopoietic stem and progenitor cells. Blood 1998;92:894–900.
20. Austin RJ, Straube J, Bruedigam C, et al. Distinct effects of ruxolitinib and interferon-alpha on murine JAK2V617F myeloproliferative neoplasm hematopoietic stem cell populations. Leukemia 2020;34:1075–89. https://doi.org/10.1038/s41375-019-0638-y.
21. Thaw K, Harrison CN, Sriskandarajah P. JAK inhibitors for myelofibrosis: strengths and limitations. Curr Hematol Malig Rep 2024;19:264–75. https://doi.org/10.1007/s11899-024-00744-9.
22. Matucci A, Maggi E, Vultaggio A. Mechanisms of action of Ig preparations: immunomodulatory and anti-inflammatory effects. Front Immunol 2015;5:690. https://doi.org/10.3389/fimmu.2014.00690.
23. Issekutz AC, Rowter D, Macmillan HF. Intravenous immunoglobulin G (IVIG) inhibits IL-1- and TNF-α-dependent, but not chemotactic-factor-stimulated, neutrophil transendothelial migration. Clin Immunol 2011;141:187–96. https://doi.org/10.1016/j.clim.2011.08.003.
24. Papayannopoulou T, Brice M. Integrin expression profiles during erythroid differentiation. Blood 1992;79:1686–94.
25. Socolovsky M, Nam H, Fleming MD, Haase VH, Brugnara C, Lodish HF. Ineffective erythropoiesis in Stat5a−/−5b−/− mice due to decreased survival of early erythroblasts. Blood 2001;98:3261–73.
26. Ulyanova T, Jiang Y, Padilla SM, Papayannopoulou T. Erythroid cells generated in the absence of specific $\beta1$-integrin heterodimers accumulate reactive oxygen species at homeostasis and are unable to mount effective antioxidant defenses. Haematologica 2013;98:1769–77. https://doi.org/10.3324/haematol.2013.087577.
27. Cheng HW, Onder L, Novkovic M, et al. Origin and differentiation trajectories of fibroblastic reticular cells in the splenic white pulp. Nat Commun 2019;10:1739. https://doi.org/10.1038/s41467-019-09728-3.
28. Perez OA, Yeung ST, Vera-Licona P, et al. CD169 + macrophages orchestrate innate immune responses by regulating bacterial localization in the spleen. Sci Immunol 2017;2:eaah5520. https://doi.org/10.1126/sciimmunol.aah5520.
29. An H, Huang Y, Zhao Z, et al. Splenic red pulp macrophages eliminate the liver-resistant *Streptococcus pneumoniae* from the blood circulation of mice. Sci Adv 2025;11:eadq6399. https://doi.org/10.1126/sciadv.adq6399.
30. Yamamoto H, Ehling M, Kato K, et al. Integrin $\beta1$ controls VE-cadherin localization and blood vessel stability. Nat Commun 2015;6:6429. https://doi.org/10.1038/ncomms7429.

Supplementary Table E1A In vivo treatment antibodies

antibody	Name	clone	isotype	company	Cat-Nr.	RRID
anti-VLA-4-antibody (β_1-integrin)	InVivoMAb anti-mouse/human VLA-4 (CD49d)	PS/2	Rat IgG2bκ	BioXCell	BE0071	AB_1107657
IgG-isotype-control (for anti-VLA-4)	InVivoMAb rat IgG2b isotype control	LTF-2	Rat IgG2bκ	BioXCell	BE0090	AB_1107780
anti-CD18-antibody (β_2-integrin)	Purified NA/LE Rat anti-mouse CD18 GAME-46 (RUO)	GAME-46	Rat IgG1κ	BD Pharmingen™	555280	AB_395703
IgG-isotype-control (for anti-CD18)	Purified NA/LE Rat IgG1κ isotype control	R3-34	Rat IgG1 κ	BD Pharmingen™	553921	AB_395136

Supplementary Table E1B FACS and MELC antibodies

antibody	clone	label	dilution	company	Cat-Nr.	RRID
B220	RA3-6B2	biotin	1:100	Biolegend	103204	AB_312989
Ter119	TER-119	biotin	1:100	Biolegend	116204	AB_313705
Gr1	RB-8C5	biotin	1:100	Biolegend	108404	AB_313369
CD3	17A2	biotin	1:100	Biolegend	100244	AB_2563947
CD4	GK1.5	biotin	1:100	Biolegend	100404	AB_312689
CD5	53-7.3	biotin	1:100	Biolegend	100603	AB_312732
CD8	53-6.7	biotin	1:100	Biolegend	100704	AB_312743
CD19	6D5	biotin	1:100	Biolegend	115504	AB_313639
CD127	A7R34	biotin	1:100	Biolegend	135006	AB_2126118
CD11b	M1/70	PerCP	1:100	Biolegend	101229	AB_2129375
CD16/32	93	Alexa Fluor 647	1:100	Biolegend	101314	AB_2278396
CD29	HMβ1-1	Alexa Fluor 488	1:120 (MELC)	Biolegend	102212	AB_492829
CD34	RAM34	FITC	1:33	BD	553733	AB_395017
CD71	R17217 (RI7 217.1.4)	APC	1:100 1:480 (MELC)	Invitrogen	17-0711-82	AB_1834355
CD157	BP-3	PE	1:480 (MELC)	Biolegend	140204	AB_10642685
CD169	3D6.112	APC	1:120 (MELC)	Biolegend	142417	AB_2565640
c-kit (CD117)	2B8	APC-Cy7	1:100	Biolegend	105826	AB_1626278
F4/80	BM8	Alexa488	1:480 (MELC)	eBioscience	53-4801-82	AB_469915
Ly-6A/E (Sca-1)	D7	Pe-Cy7	1:100	Biolegend	108114	AB_493596
Ly6-C	HK1.4	BV421	1:100	Biolegend	128032	AB_2562178
Ly6-G	1AS	BV510	1:100	Biolegend	127633	AB_2562937
Propidium-iodide			1:5000 (MELC)	Sigma-Aldrich	537060	
Ter119	TER-119	PE	1:100 1:240 (MELC)	Biolegend	116207	AB_313708
Streptavidin		BV421	1:100	Biolegend	405226	